Stages in Iron Storage in the Ferritin of *Escherichia coli* (EcFtnA): Analysis of Mössbauer Spectra Reveals a New Intermediate†

Erika R. Bauminger,*,‡ Amyra Treffry,§ Michael A. Quail,§,|| Zhongwei Zhao,§,⊥ Israel Nowik,‡ and Pauline M. Harrison§

Racah Institute of Physics, The Hebrew Universuty, Jerusalem 91904, Israel, and The Krebs Institute, Department of Molecular Biology and Biotechnology, University of Sheffield, England

Received February 16, 1999; Revised Manuscript Received April 20, 1999

ABSTRACT: Iron uptake into the nonheme ferritin of *Escherichia coli* (EcFtnA) and its site-directed variants have been investigated by Mössbauer spectroscopy. EcFtnA, like recombinant human H chain ferritin (HuHF), oxidized Fe(II) at a dinuclear ferroxidase center situated at a central position within each subunit. As with HuHF, Mössbauer subspectra observed between 1 min and 24 h after Fe(II) addition were assigned to Fe(III) monomers, "c", μ-oxo-bridged dimers, "b", and clusters, "a", the latter showing magnetically split spectra, "d", at 4.1 K. Like those of HuHF, the μ-oxo-bridged dimers were formed at the ferroxidase centers. However, the analysis also revealed the presence of a new type of dimer, "e" ($QS_1 = 0.38$ mm/s, $IS_1 = 0.51$ mm/s and $QS_2 = 0.72$ mm/s, $IS_2 = 0.50$ mm/s), and this was also assigned to the ferroxidase center. Dimers "b" appeared to be converted to dimers "e" over time. Subspectra "e" became markedly asymmetric at temperatures above 90 K, suggesting that the two Fe(III) atoms of dimers "e" were more weakly coupled than in the μ-oxo-bridged dimers "b", possibly due to OH^- bridging. Monomeric Fe(III), giving relaxation spectra "c", was assigned to a unique site C that is near the dinuclear center. In EcFtnA all three iron atoms seemed to be oxidized together. In contrast to HuHF, no Fe(III) clusters were observed 24 h after the aerobic addition of 48 Fe(II) atoms/molecule in wild-type EcFtnA. This implies that iron is more evenly distributed between molecules in the bacterial ferritins, which may account for its greater accessibility.

Iron is found in virtually all living organisms where it performs a variety of essential roles. However, in aerobic environments, free iron is also toxic and the widespread occurrence of the iron-sequestering protein, ferritin, is a natural response to those conflicting characteristics. Two classes of ferritin are known in bacteria: hemoferritins, usually known as bacterioferritin (Bfr), and nonheme ferritins, designated Ftn (*1*). Animal ferritins are nonheme, as isolated. Many of them, for example, human ferritin, are heteroplymers of two chains called H and L, which have complementary roles in iron storage: H chains catalyze Fe(II) oxidation and L chains promote the growth of Fe(III) clusters (*1*).

The structures of ferritins from a wide range of species have been determined. They have a common architecture, being built from twenty-four polypeptide chains folded into equivalent 4-helix bundles and arranged in 432 symmetry to give a hollow shell (*1*−*3*). The central 80 Å diameter cavity allows up to 4500 Fe(III) atoms to be stored as an inorganic complex or "iron core" (*1*).

Three iron-storage proteins are known in *Escherichia coli:* a "bacterioferritin" (EcBfr)[1] and two nonheme ferritins, EcFtnA and EcFtnB. EcFtnB has been identified only from its primary structure, which resembles that of EcFtnA (*3*). However some of the residues critical for fast iron oxidation, which are found in EcFtnA and EcBfr, are missing from EcFtnB and its function is unknown. It is unlikely to form heteropolymers with either EcBfr or EcFtnA, as the residues involved in intersubunit interactions in these ferritins are not conserved in EcFtnB.

EcBfr and EcFtnA have been isolated and their crystal structures determined (*3*−*5*). Three iron-binding sites (per subunit) have been identified in EcFtnA (Figure 1), two (A and B) at a dinuclear center within the 4-helix bundle and a third (C) nearby on the inner surface of the protein shell (*5*). These iron sites also bind Tb^{3+} and Zn^{2+}. A dinuclear metal center, probably occupied by Mn^{2+} ions, has been located at an equivalent position in EcBfr (*4*), and two Tb^{3+} ions have been found to bind in similar sites in human ferritin H chains (HuHF) (*6*). Aided by site-directed mutagenesis, evidence has accumulated for the involvement of the dinuclear centers in the catalytic oxidation of a pair of Fe(II) atoms in all three *ferritins* (*1*, *7*−*10*). Studies with recom-

† This research was supported by the Welcome Trust, England.

* Phone: 972-2-6584744. Fax: 972-2-6586347. E-mail: Erika@vms.huji.ac.il.

‡ The Hebrew University.

§ University of Sheffield.

|| Current address: Sanger Centre, Hinxton Hall, Cambridge, CB10 1SA, U.K.

⊥ Current address: Dept. of Biochemistry, 474 Medical Science Building, University of Alberta, Edmonton, Alberta TG6 2H7, Canada.

[1] Abbreviations: EcFtnA, *E. coli* nonheme FtnA ferritin; HuHF, recombinant human H chain ferritin; EcBfr, *E. coli* bacteria hemoferritin; FrHF, recombinant frog H ferritin; FrMF, recombinant frog M ferritin; WT, wild type; HoSF, horse spleen ferritin; QS, quadrupole splitting; IS, isomer shift.

10.1021/bi990377l CCC: $18.00
Published on Web 05/20/1999

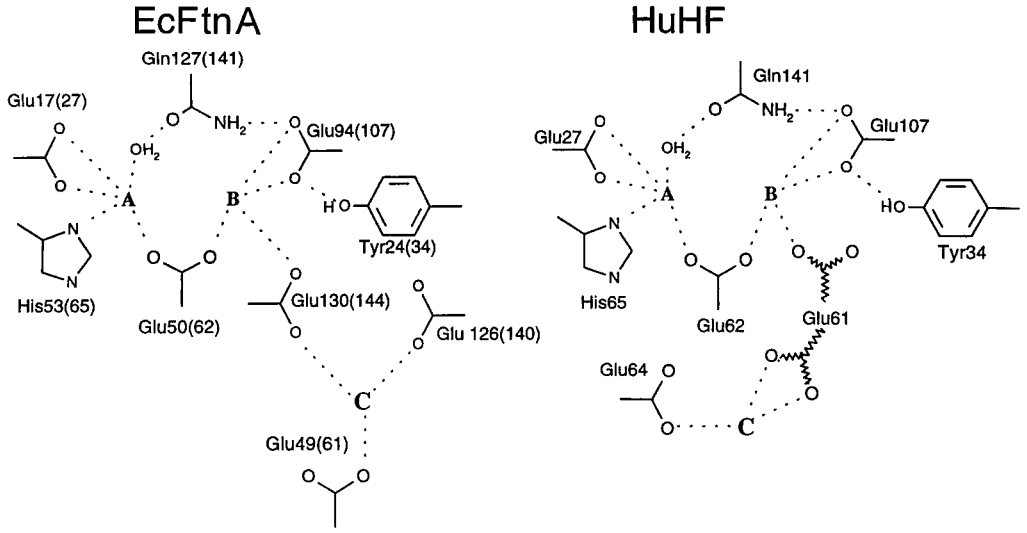

FIGURE 1: Schematic diagrams depicting the metal binding centers of EcFtnA (left) and HuHF (right).

binant frog H (FrHF) and M (FrMF) ferritins also indicated the concomitant oxidation of two Fe(II) atoms (*11*). Recent spectroscopic evidence indicates that oxidation proceeds via a diferric peroxo intermediate (*1*, *9*, *12*, *13*).

In all H-type ferritins (including EcFtnA), in vitro studies indicate that the initial catalytic oxidation of two Fe(II) atoms/molecule represents the first of a complex series of steps leading to iron storage as the mineral ferrihydrite or ferric phosphate (*9*, *10*, *12*−*16*). However, despite obvious structural similarities between the ferritins, both the dinuclear sites themselves and the Fe(II) oxidation products of EcFtnA, EcBfr, HuHF, and FrHF show differences in detail. Unlike HuHF, in EcFtnA the initial oxidation of Fe(II) in the dinuclear center is accompanied by oxidation of a third Fe(II) atom (*16*, *17)*. Preliminary Mössbauer spectroscopic analyses (*18*) showed differences in the relative proportions of oxidation products (Fe(III) dimers, monomers, and clusters) and the presence of a novel quadrupole doublet in EcFtnA, not seen in HuHF. In FrHF three dimers and a trimer, all originally thought to be associated with tyrosine, were described as the initial oxidation products (*15*) although in later studies these were considered to have arisen post-oxidation (*11*, *13*).

It is perhaps not surprising that EcFtnA and HuHF behave differently, given that their overall identity in primary structures is only 22%. Nevertheless their dinuclear centers are strikingly similar (Figure 1) in that two site A ligands, Glu17/27 and His53/65 (EcFtnA and HuHF sequence numbering respectively), the bridging ligand (Gln50/62), and one of the site B ligands (Glu94/107) are at equivalent positions in the aligned primary structures and similarly disposed in the three-dimensional structures. However, the third of site B ligands are not the same (Glu130 in EcFtnA instead of Glu61 in HuHF), and the two C sites are quite different (ligands Glu49, Glu126, and Glu130 in EcFtnA or Glu61 and Glu64 in HuHF[2]).

Events following aerobic addition of Fe(II) to wild-type EcFtnA (WT) and its variants (E17A, Y24F, E49A, E50A, E94A, E126A, and E130A; see Figure 1) have now been analyzed in detail by measuring Mössbauer spectra of samples frozen at various times after the addition of Fe(II) as $^{57}FeSO_4$. The slow oxidation observed with variants E94A, E17A, E50A, and Y24F supports the conclusion that Fe(II) oxidation occurs initially at the dinuclear center in this ferritin, as in HuHF. Analyses of spectra of EcFtnA samples, like those of HuHF, also indicate that Fe(III) oxo-bridged dimers are formed at the dinuclear centers within less than 1 min after Fe(II) addition. As well as the four subspectra observed in HuHF (*7*, *8*, *18*), a unique additional doublet, "e", was observed in EcFtnA. Analysis of this novel spectrum, "e", suggests that it is due to a second dimer (probably hydroxo-bridged) also situated at the ferroxidase center. Over time the percentage of this dimer seems to grow at the expense of the oxo-bridged Fe(III) dimer. The significance of the presence of species "e" is discussed here.

A preliminary examination has also been made of a few samples frozen at 10 s, some of which (E49A and E130A) contain a previously reported (*12*) transient blue complex. Analyses of these spectra are described.

MATERIALS AND METHODS

Site-Directed Mutagenesis and Protein Purification. EcFtnA overexpression and production of site-directed variants were carried out using the expression vector pALTER-Ex1, as supplied bPromega UK (Southampton, England). Ferritins were purified according to Hudson et al. (*19*) with minor modifications (*10*). The purification procedure yielded iron-free proteins.

Protein concentrations were determined with the Bio-Rad reagent. The color response was standardized using an EcFtnA sample whose concentration had been determined by amino acid analysis.

Sample Preparation for Mössbauer Spectroscopy. $^{57}FeSO_4$ solutions were prepared as described by Bauminger et al. (*20*). Most samples were prepared using 1 mL of 5.63 μM protein in 0.1 M Mes buffer, pH 6.5, and 5 mM NaCl, by adding $^{57}FeSO_4$ to give a final concentration of 0.27 mM in Fe(II) (48 Fe(II) atoms/molecule). Some samples were prepared in the same way except that Fe(II) was 1 mM and protein 20.8 μM. Samples were frozen in liquid N_2 at the specified times (t_f) after iron addition and kept in liquid nitrogen until measurements were performed.

[2] The sequence numbers used are the actual positions in the primary structures; Glu 49 in EcFtnA and Glu61 in HuHF are at equivalent positions.

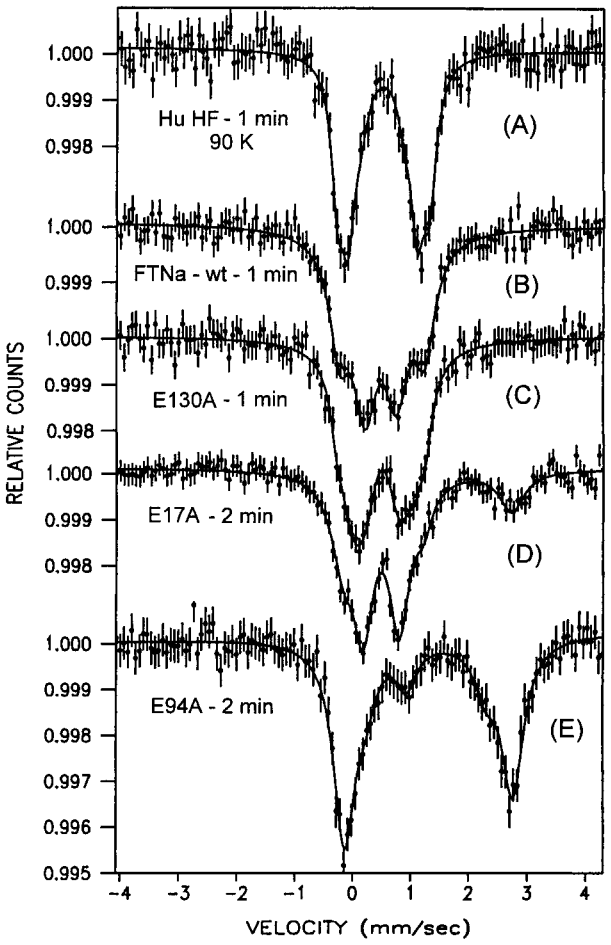

FIGURE 2: Mössbauer spectra obtained at 90 K in HuHF and EcFtnA and some of its variants, frozen 1 or 2 min after addition of 48 Fe atoms/molecule.

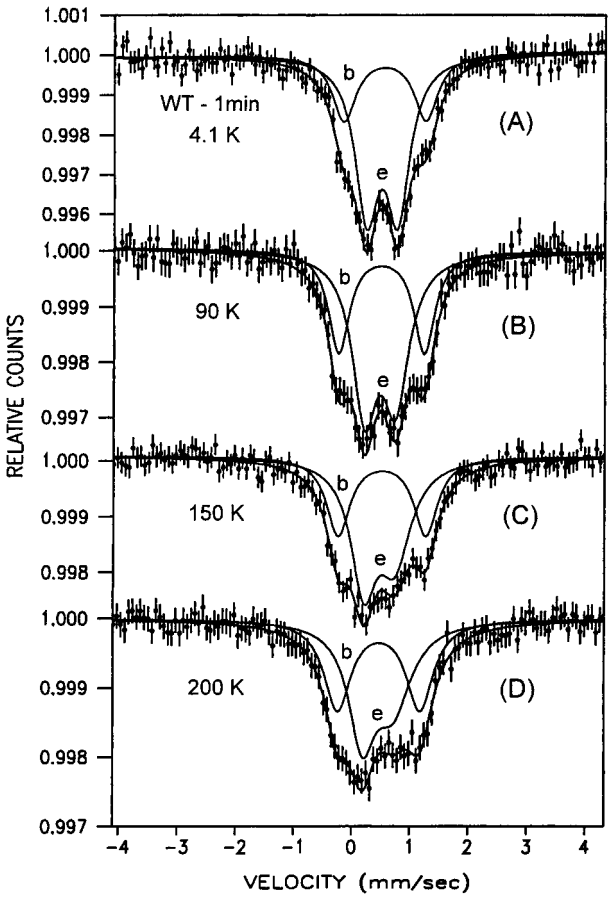

FIGURE 3: Spectra obtained at different temperatures in EcFtnA-wt, frozen 1 min after addition of 48 Fe atoms/molecule, showing the change of the spectral shape with temperature. For simplicity only one average doublet for dimer "b" and one for dimer "e" is shown.

Samples were analyzed by conventional Mössbauer spectroscopy with a 100 mCi ^{57}Co(Rh) source, held at room temperature. A Harwell proportional counter was used. Velocity calibration was performed with a metallic iron foil at room temperature. Isomer shifts are quoted with respect to this absorber. Spectra from all samples were obtained at 90 K, and from most of the samples spectra were also measured at 4.1 K in two velocity ranges. Some samples were also measured at higher temperatures (up to 200 K). Least-squares computer fits were performed to all measured spectra, using Lorentzian line shapes. A simple relaxation model with one hyperfine field and one relaxation time was used to fit relaxation spectra (*21*). Mössbauer parameters and relative intensities of all subspectra were obtained from these fits.

RESULTS

Mössbauer Spectra and Their Analysis. Mössbauer spectra obtained at 90 K with WT and selected variants, frozen at either 1 or 2 min after loading with 48 Fe atoms/molecule, are shown in Figure 2 and compared with HuHF loaded similarly. It is obvious that very different spectra were obtained with the different variants. The effect of temperature on spectra obtained with WT samples frozen 1 min after iron loading with 48 Fe(II) atoms/molecule is shown in Figure 3. Most spectra were symmetric at 4.1 K, slightly asymmetric at 90 K, but became very asymmetric at higher temperatures. The increase in asymmetry with temperature was even more pronounced with some variants. In E130A, for example, the change in the spectral shape between 4.1 and 90 K is striking (Figure 4). Over a larger velocity range, the spectra of most samples measured at 90 K also showed slow relaxation spectra, "c", extending to about ±8 mm/s (Figure 5A). At 4.1 K these relaxation subspectra were better defined, due to somewhat slower relaxation at this temperature (Figure 5B). However, their contribution to the central part of the Mössbauer spectra measured at a lower velocity range (±4 mm/s) was small and may be neglected in the computer fitting procedures. All spectra obtained at 4.1 K, at the low velocity range, could be interpreted as a number of superimposed symmetric doublets. In some cases the contribution of a magnetically split sextet to the spectra measured at this velocity range had to be taken into account. At the larger velocity range a magnetically split sextet, "d", was also observed in some samples. Such a magnetic subspectrum was seen in WT samples with more than 48 Fe atoms/molecule (Figure 5C) and in some variants with only 48 Fe atoms/molecule. In variants with slow rates of oxidation, subspectra corresponding to Fe(II), with isomer shift (IS) between 1.27 and 1.34 mm/s, were also present (e.g., Figure 2D,E).

Analyses of the Mössbauer data have to account for the spectra observed both at 4.1 K and at higher temperatures. A rough fit to the central part of spectra, obtained at 4.1 K

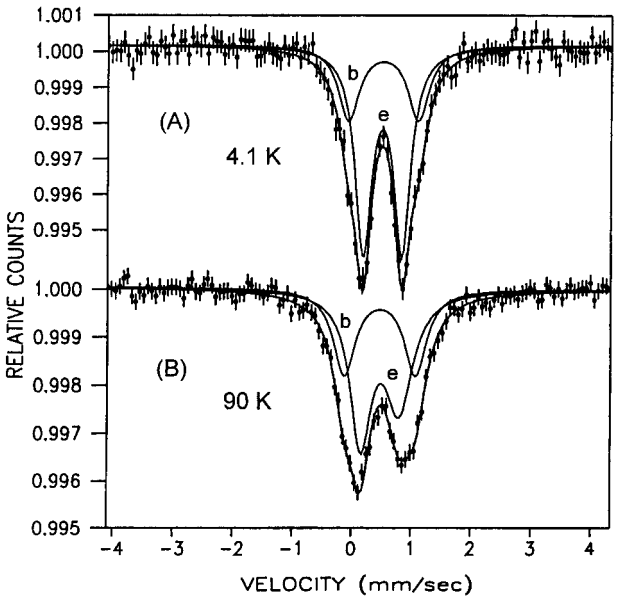

FIGURE 4: Spectra obtained at 4.1 and 90 K in E130A frozen 10 min after adding 48 Fe atoms/molecule. The spectrum, which is symmetric at 4.1 K, is very asymmetric at 90 K. "e" and "b" are as in Figure 3.

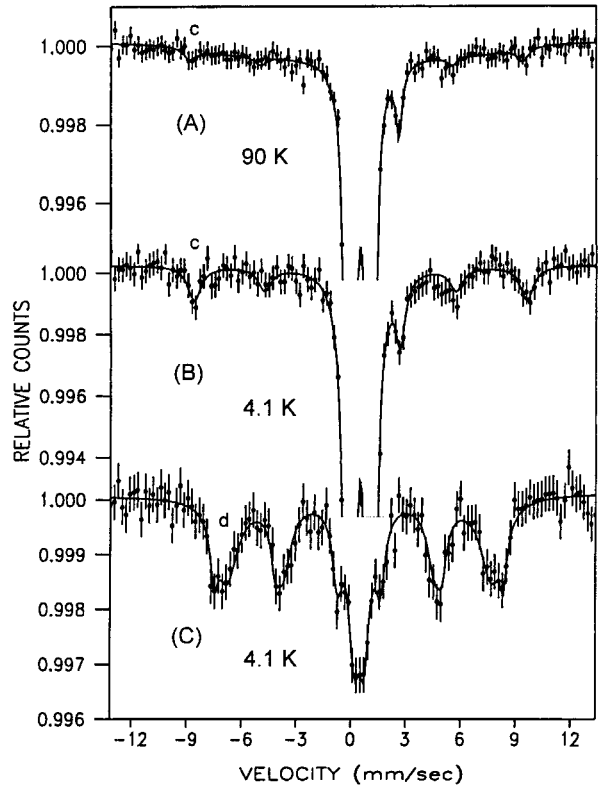

FIGURE 5: Spectra extending to larger velocities, obtained at (A) 90 K and (B) 4.1 K in WT frozen 10 s after the addition of 48 Fe atoms/molecule (1 mM) and (C) obtained at 4.1 K in WT frozen 24 h after addition of 144 Fe atoms/molecule. The relaxation sub-spectrum "c", which is very smeared out at 90 K (A), shows sharper lines at 4.1 K. (C) shows the magnetically split sub-spectrum "d" due to clusters in this sample.

and measured at a velocity range of ±4 mm/s, could be obtained with two doublets with somewhat broadened lines. In WT (Figure 3), one of these doublets showed a quadrupole splitting (QS) of around 1.4 mm/s (doublet "b"), and the other had a QS of about 0.53 mm/s (doublet "e"). As can be seen in Figure 3, the shape of doublet "b" was independent of temperature, whereas doublet "e" became very asymmetric at higher temperatures.

What could cause spectra to be symmetric at 4.1 K and asymmetric at higher temperatures? Texture effects can be excluded, since they should be temperature-independent, as well as Goldanskii-Karyagin (G-K) effects, which are extremely unlikely to be found at these low temperatures due to the high *f*-factor of the 14.4 keV radiation of ^{57}Fe (*22*). Moreover, a G-K effect would lead to higher asymmetry as temperatures are raised, whereas the spectral asymmetry given by some samples, such as E130A, was unchanged between 90 and 200 K (the highest temperature at which spectra were measured). A symmetric doublet at 4.1 K, which shows asymmetry at higher temperatures, can therefore be due only to faster relaxation at 4.1 K than at 90 K. Such relaxation phenomena could have been produced in one of two ways, both yielding very similar Mössbauer spectral shapes:

(1) For an isolated Fe(III) monomer, the crystal field may split the $^6S_{5/2}$ ground state in such a way that the $\pm^1/_2$ levels lie lowest in energy. The relaxation time in these states is much faster then those of the $\pm^3/_2$ and $\pm^5/_2$ levels. Thus if only the $\pm^1/_2$ levels are populated at 4.1 K, a pure symmetric doublet will be observed at this temperature, whereas at higher temperatures, as the other levels become populated, the slower relaxation will cause asymmetry. This phenomenon was first observed by Shulman and Wertheim for ferric hemin (*23*) and interpreted by Blume (*24*) and has since been observed in many compounds (e.g., see ref *25*). In all cases hitherto observed, such spectra were already asymmetric at 90 K. The temperature at which asymmetry appears will depend on the crystal field splitting and for iron this splitting is expected to be small, and hence at 90 K these spectra are all expected to be asymmetric. The fact that the temperature at which asymmetry appears is very different in the different variants, and in some of them the spectra at 90 K are still symmetric, makes this mechanism very unlikely in the present case.

(2) In an antiferromagnetically coupled Fe(III) dimer, the two $S = {}^5/_2$ spins of the iron atoms may couple to produce multiplets with $S' = 0, 1, 2, \ldots 5$. At 4.1 K only the $S' = 0$ ground state is populated, and in the Mössbauer spectrum, either one or two symmetric doublets will be observed, depending on whether the two iron atoms are equivalent. As the temperature is raised, higher multiplets may become populated and relaxation phenomena will be observed, causing the doublets to acquire an asymmetric shape. Such a phenomenon has been observed in $(Fe(salen)Cl)_2$ and several other Schiff base complexes (*26*, *27*). The temperature at which the doublets become asymmetric depends in this case on the strength of the antiferromagnetic coupling between the two Fe^{3+} atoms, which determines the splitting between the S' multiplets (*27*). This temperature may vary to a large extent (for example, the $S' = 1$ level lies at about 20 K in $(Fe(salen)Cl)_2$ and at about 300 K in $(Fe(salen)_2O)$. This leads to the conclusion that this is the mechanism responsible for the observed phenomena. Confirmation of this interpretation is provided by a high-field (14 T) Mössbauer measurement of a WT sample frozen 10 s after iron loading (1 mM). This measurement showed that about 70% of the iron atoms were in the form of dimers with

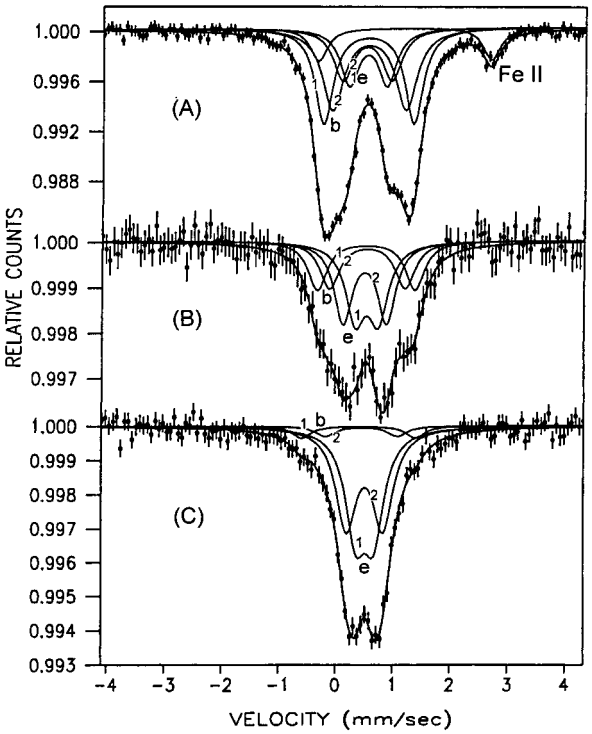

FIGURE 6: Spectra obtained in WT samples obtained at 4.1 K and frozen at different times t_f after the addition of 48 Fe atoms/molecule: (A) $t_f = 10$ s (1 mM); (B) $t_f = 30$ s (0.27 mM); and (C) $t_f = 1$ h (0.27 mM). Note the change in relative intensities between doublets "b" and doublets "e", as well as a change in QS of "e". (Two doublets are shown for "e" ("e_1" and "e_2") and two for "b" ("b_1" and "b_2")).

magnetic coupling to give an $S' = 0$ diamagnetic state at 4 K. The spectra showed that more than one kind of dimer species were present, yet separation into the different dimer species was not possible (D. P. E. Dickson, private communication).

An exact analysis of relaxation spectra demands a superposition of relaxation spectra from all of the different multiplets, yet line shapes which are phenomenologically identical, within the accuracy of the experimental spectra, will be obtained using a simple relaxation model, based on relaxation between two spin states only (*21*). In such an analysis an arbitrary hyperfine field can be chosen, and values for relaxation times will then depend on the chosen field. Though these analyses will not yield the true values for relaxation times, they allow computer fits to experimental spectra to be calculated. These fits will give the correct values for the relative intensities of the subspectra and will enable comparison between different spectra. In this way shorter relaxation times obtained at a given temperature will indicate a larger splitting between the S' multiplets and imply a stronger coupling between the two Fe^{3+} ions. As can be seen in Figures 3 and 4, the simple relaxation model yields very good fits to the experimental spectra.

In a more refined analysis of the spectra obtained at 4.1 K, each of doublets "b" and "e" were split into two doublets, which were constrained to be of equal intensity (Figure 6). Their parameters are given in Table 1. Those of doublets "b" are likely to be due to an oxo-bridged Fe(III) dimer. Moreover, the finding that subspectra "b" were not observed in variant E50A in which the bridging carboxyl ligand is absent suggests that they are due to an Fe(III) dimer at the chemically distinct sites A and B (Figure 1). In previous analyses of spectra obtained in HuHF (*7*, *8*, *18*) and also in EcFtnA (*18*), doublets with similar parameters were not constrained to be equal, implying that they are due to two distinct dimers, each with two equivalent sites. However reanalyses with the constraint of equal intensity of the two "dimer" doublets "b_1" and "b_2" of all previously obtained spectra gave equally good fits without producing a significant change in the relative intensity of subspectra "b" compared with other species. The new interpretation is therefore considered more likely. In spectra obtained at 90 K these doublets were the same as at 4.1 K, showing the same QS and a slight change of about 0.02 mm/s in IS, consistent with a second-order Doppler shift (*29*).

In most variants, one of doublets "e" ("e_1") showed a much smaller QS than any observed before with HuHF. Doublet "e_2" showed QS and IS very similar to those of doublet "a", which in HuHF has been assigned to small nonmagnetic clusters (*7*, *8*, *18*). The spectra obtained at temperatures of 90 K or more were analyzed with doublets showing the same QS as at 4.1 K, but doublets "e" were allowed to relax to give the observed asymmetry. Following the interpretation given above, doublets "e" were attributed to dimers "e", with weaker coupling between the two iron atoms than with the oxo-bridged dimers "b". In those cases in which the magnetically split subspectrum "d" was observed at 4.1 K, an additional doublet "a" of equal relative intensity to "d" was observed at 90 K. This doublet, which had parameters QS = 0.75 mm/s and IS = 0.49 mm/s at 90 K, was attributed to Fe(III) in small clusters which were superparamagnetic at 90 K.

As mentioned above, a slow relaxation spectrum "c", attributed, as in HuHF, to Fe(III) monomers, was also observed in WT and most variants at 90 K. However, the finding that this subspectrum was not detected (or was very weak) in variants E49A and E126A (site C ligands, Figure 1) suggests that it is mainly due to iron in site C. In the spectra of most variants measured at 4.1 K, subspectrum "c" could not be distinguished from subspectrum "d", both extending to velocities of about ±8 mm/s. Such spectra were fit with a single composite magnetically split subspectrum with broadened lines. At 90 K the only subspectrum extending over the velocity range up to ±8 mm/s was subspectrum "c" and the magnetically split subspectrum given by clusters was replaced by doublet "a". To deconvolute the relative intensity of subspectrum "d" at 4.1 K from subspectrum "c", we subtracted the relative intensity of the latter (obtained from the 90 K spectra) from the relative intensity of the complete magnetically split spectrum observed at the lower temperature. Computer fits to all measured spectra yielded the parameters given in Table 1. The percentage of iron in each species, after the addition of 48 Fe(II) atoms/molecule, is given in Table 2; the assignment is based on the relative intensities of the various subspectra. In Tables 3 and 4 the data are expressed as the number of iron atoms in each site, following the additions of more than 48 Fe(II) atoms/molecule; again the assignment is derived from the relative intensities of the various subspectra (the number of atoms in dimers was rounded to give an even number).

In some variants (E50A, E94A, and E126A; Table 1) the parameters of dimer doublets "e" were very similar to the

Table 1: Mössbauer Parameters of Dimers "b" and "e"[a]

	dimer (b) (4.1 K)				dimer (e) (4.1 K)				dimer (e)
	$QS(b_1)$, mm/s	$IS(b_1)$, mm/s	$QS(b_2)$, mm/s	$IS(b_2)$, mm/s	$QS(e_1)$, mm/s	$IS(e_1)$, mm/s	$QS(e_2)$, mm/s	$IS(e_2)$, mm/s	T_{rel} (90 K) ($\times 10^{-9}$), s[b]
HuHF	1.23	0.50	1.56	0.52			0.75	0.49	<0.008
EcFtnA-WT[c]	1.34	0.53	1.65	0.52	0.38	0.51	0.72	0.50	0.017
E94A							0.75	0.51	<0.008
E17A	1.22	0.53	1.51	0.55	0.42	0.51	0.71	0.48	0.017
E50A							0.74	0.53	<0.008
Y24F[d]	1.38	0.57	1.70	0.58	0.38	0.49	0.71	0.49	<0.008
E130A	1.13	0.54	1.43	0.53	0.51	0.49	0.78	0.50	0.025
E49A[e]	1.16	0.52	1.57	0.54	0.51	0.47	0.84	0.48	<0.008
E126A	1.14	0.56	1.49	0.55			0.80	0.50	<0.008

[a] The errors on each number are ±0.02 mm/s; the line widths were in all cases less than 0.5 mm/s. [b] With arbitrarily assumed hyperfine field of 55 tessla. [c] In fast frozen samples of WT, at 30 s (set one), parameters of "e" are the following: QS(e) = 0.66 and 0.85 and IS(e) = 0.53 and 0.52 mm/s. [d] In early Y24F (until t_f = 2 min), parameters of "e" are the following: QS(e) = 0.55 and 0.84 and IS(e) = 0.49. The parameters of Fe(II) are the following: QS = 2.76 and IS = 1.20 mm/s. [e] There is a small but significant difference in doublets "b" parameters in samples with 1 mM Fe (set one) and those with 0.27 mM (set two). As samples prepared with 1 mM were frozen at $t_f \leq 1$ min, it is hard to know whether this change is due to a difference in t_f or Fe(II) concentration. With 1 mM Fe the parameters are the following: QS(b) = 1.12 and 1.43 mm/s and IS(b) = 0.55 mm/s.

Table 2. Percentages of Iron in Dimers, "b" and "e", Monomers, "c", Clusters, "d", and as Fe(II) in EcFtnA and Variants, at Various Times after the Addition of 48 Fe(II) Atoms/Molecule (0.27 mM Fe(II)) at 25 °C[a]

variant	t_f	% b	% e	% c	% d	% Fe(II)
WT	10 s[b]	42	21	30		7
	60 s[b]	37	43	20		
	30 s	30	45	25		
	1 min	26	44	30		
	2 min	22	48	30		
	1 h	12	58	30		
	24 h	12	53	35		
E94A	30 s		30	10		60
	2 min		18	20		62
	1 h		14	38		48
	4 h	5	20	45		30
	24 h		14	30	38	18
E17A	2 min	6	31	30	20	13
	1 h	5	50	25	20	
	24 h	6	49	25	20	
E50A	10 s[b]		13	5	9	73
	1 min		7	20	22	51
	1 h		20	10	60	10
Y24F	1 min	11	59	20		10
	1 h	18	52	30		
	24 h	18	60	30		
E130A	10 s[b]	49	41	10		
	1 m[b]	29	61	10		
	2 min	29	47	25		
	1 h	7	23	25	45	
	24 h				100	
Y24F	1 min	11	59	20		10
	1 h	18	52	30		
	24 h	18	60	30		
E49A	1 min	50	50			
	1 h	29	31		40	
	24 h	10			90	
E126A	1 min	60	40			
	24 h	27	33		40	

[a] Errors on All ±5 %. [b] Sample prepared at 6 °C with 1 mM Fe(II).

Table 3. Number of Iron Atoms (*n*) in Each Species, in EcFtnA and Some Variants, after Loading with More than 48 Fe(II) Atoms/Molecule[a]

variant	t_f	*n* ("b")	*n* ("e")	*n* ("c")	*n* ("d")[b]	*n* (Fe(II))
			96 Fe Atoms/Molecule			
WT	2 min	26	16	24	30	
	1 h	2	36	20	38	
	2 h	4	20	18	54	
E17A	15 min	8	40	8	24	16
	1 h	14	34	24	24	
	2 h	10	38	24	24	
	24 h	6	14	24	52	
E50A	1 h			17	67	12
Y24F	2 min	24	22	24	20	6
	1 h	10		24	62	
	24 h	4		24	68	
E130A	2 min	14	28	14	40	
	1 h				96	
E49A	1 h	8			88	
E126A	1 h	12	12		72	
			144 Fe Atoms/Molecule			
WT	3 min	20	12	14	98	
	24 h	6	26		112	
E17A	15 min	10	36	22	4	72
	24 h	6	42	22	74	
Y24F	3 min	30	10	22	79	3
	24 h			22	122	
E130A	3 min				144	

[a] Error on *n*: ±2. [b] Average number.

parameters of doublet "a", assigned previously to clusters. In these cases it was impossible to distinguish between dimer doublets "e" and cluster doublet "a" at 90 K and between these dimers and nonmagnetic clusters at 4.1 K. It was previously assumed (*7*, *8*) that doublet "a" seen at 4.1 K is due to clusters which are too small to give magnetically split spectra due to superparamagnetism. It is now postulated that all doublets observed at 4.1 K are due mainly to dimers. This hypothesis is based on the finding that in variants in which dimers "e" showed different parameters from those of the cluster doublet, no cluster doublet "a" was observed at 4.1 K. Pereira et al. (*15*) also observed a dimer in frog ferritin with parameters similar to those of doublet "a", and the doublet assigned previously to small clusters, "a", in HuHF (*7*, *8*, *18*) may also be mainly due to a dimer. However, asymmetric spectra were not observed in HuHF or in most of its variants at 90 K, indicating that if this doublet was due to a dimer, the coupling of the two iron atoms comprising this dimer was stronger in HuHF than in dimers "e" of EcFtnA. Symmetric spectra at 4.1 K and asymmetric spectra at 90 K were observed in only one HuHF variant (Q141E) (unpublished observation), indicating a weaker coupling of the two iron ions in this HuHF variant.

Table 4. The Fate of Two Separate Additions of Fe(II) to EcFtnA[a]

no.		*n* ("b")	*n* ("e")	*n* ("c")	*n* ("d")[b]
	A. Effect of Pre-existing Fe(III) on the Species Distribution of a Second Addition of 48 Fe(II) Atoms/Molecule (Number of ^{57}Fe Atoms)				
1	^{57}Fe-1 min	12	20	16	
2	48^{56}Fe-1 min + ^{57}Fe-1 min	10	6	10	22
3	48^{56}Fe-1 min + ^{57}Fe-1 h	2	16	7	23
4	48^{56}Fe-1 h + ^{57}Fe-1 min	2	16	5	25
5	48^{56}Fe-1 h + ^{57}Fe-1 h			4	44
6	144^{56}Fe-24 h + ^{57}Fe-1 min	2		5	41
	B. Effect of a Second Addition of 48 Fe(II) Atoms/Molecule on Species Distribution of the First Addition of 48 Fe(II) Atoms/Molecule (Number of ^{57}Fe Atoms)				
7	^{57}Fe-2 min	10	24	14	
8	^{57}Fe-1 min + ^{56}Fe-1 min	14	16	12	6
9	^{57}Fe-1 min + ^{56}Fe-1 h	2	14	14	18
10	^{57}Fe-1 h	6	28	14	
11	^{57}Fe-1 h + ^{56}Fe-1 min	2	24	17	5
12	^{57}Fe-1 h + ^{56}Fe-1 h		12	14	22
13	^{57}Fe-1 min + ^{57}Fe-1 min	26	16	24	30
14	^{57}Fe-1 min + ^{57}Fe-1 h	2	36	20	38

[a] Errors on *n*: ±2 A. [b] Average number.

Subspectra Given by EcFtnA Samples Frozen between 10 s and 24 h after Fe(II) Addition. Two sets of WT samples containing 48 Fe atoms/molecule were examined. Both were in 0.1 M Mes buffer, pH 6.5, but samples of one set were prepared at 6 °C and a final concentration Fe(II) of 1 mM and in the second set samples were prepared at ambient temperature and a final Fe(II) concentration of 0.27 mM. Spectra measured at 90 K are shown in Figure 6A for a sample frozen at 10 s (first set) and in Figure 6B,C for samples frozen at 30 s and 1 h, respectively (second set). The sample frozen at 10 s showed traces (about 7%) of Fe(II), but in the other samples oxidation was complete. No magnetic Fe(III) clusters, "d", were observed in any of the WT samples containing only 48 Fe atoms/molecules (frozen up to 24 h). All of the spectra comprised three major components, namely doublets denoted "b" and "e" due to two types of dimer (Figure 6) and slow relaxation subspectra attributed to monomers (Figure 5A,B). The relaxation subspectra, which accounted for about 30% of the total spectrum, showed a smeared out shape at 90 K (Figure 5A) compared with a much better defined sextet at 4.1 K (Figure 5B) due to somewhat slower relaxation at this temperature. The relative proportions of "b" and "e", making up the dimer subspectra, varied over time. Doublets "b" were predominant at very early times, but they decreased in parallel with an increase in doublets "e", which became the major species by 1 min.

The parameters of the various subspectra found with WT are given in Table 1 and the percentages of iron in each species, after the addition of 48 Fe(II) atoms/molecule, are given in Table 2. At early times (t_f < 1 min), there was a significant change in the parameters of doublets "e", which may indicate the presence of an additional species (a precursor, for example, a diferric peroxo complex with a different distribution of charges around the iron atoms). Doublets "e" were slightly asymmetric at 90 K, and the asymmetry became more pronounced at higher temperatures, indicating a splitting of about 90 K between $S' = 0$ and $S' = 1$ states.

A few samples were measured with 96 or 144 Fe atoms/molecule (Table 3). In these dimers "b" were again found to decrease with time and dimers "e" to increase, and it was notable that large clusters, "d", giving magnetically split spectra at 4.1 K, were already present at 2 min. With 144 Fe atoms/molecule, at 24 h, 80% of the iron was in such clusters. In no sample was the total number of iron in dimers "b" and "e" found to exceed 48, or the number in monomers to exceed 24 per molecule.

Subspectra Given by Dinuclear Center Variants. Dinuclear center variants E17A, Y24F, E50A, E94A, and E130A were examined. E17 is a site A ligand, E50 is an A,B bridging ligand, and E94 and E130 are site B ligands, although E130 also acts as a site C ligand (Figure 1). Y24 is also situated at the dinuclear center, although it does not ligate iron. Substitutions E17A, Y24A, E50A, and E94A (and also Y24F) were all found to impede oxidation, confirming the importance of sites A and B in ferroxidase activity (Table 2 and Figure 2).

(a) Variant E94A. As expected from other studies (*10*, *16*, *17*), the substitution E94A had the most drastic effect on oxidation. About 60% of the iron was still divalent at 2 min, and even at 24 h, 18% remained unoxidized (Table 2 and Figure 2). Little or no dimer "b" was observed at any time. The parameters of doublets "e" (Table 1) are very similar to those previously attributed to nonmagnetic clusters, "a", and it is therefore impossible to distinguish between the two interpretations. However, the finding that the intensity of this doublet decreases with time, up to at least 1 h, without the formation of any large clusters (Table 2) supports the assumption that this doublet should be assigned to dimers and not to small clusters. The relative intensity of doublet "e" is always less than that observed in WT. Monomers, "c", increase with time up to 4 h and then seem to decrease as large clusters form.

In this variant at least two kinds of Fe(II) were found at all times (one with QS = 2.78 mm/s and IS = 1.31 mm/s and the other with QS = 2.44 mm/s and IS = 1.09 mm/s). Since both showed parameters different from those of free Fe(II) (QS = 3.45 mm/s, IS = 1.37 mm/s), they were probably due to Fe(II) bound to two sites on the protein with different ligands and/or different geometries.

(b) Variant E17A. Substitution of this A site ligand caused Fe(II) oxidation to slow, but to a much lesser extent than with E94A. Only 13% of the iron remained unoxidized at 2 min compared with 60% with E94A, and all was oxidized at 5 min (Table 2 and Figure 2). The parameters of this Fe(II) (QS = 2.87 and IS = 1.30 mm/s) were similar to those of one of the divalent doublets in E94A. There was very little change in the distribution of iron among the various species over the 24 h period, except during the first hour when Fe(II) disappeared and "e" increased (Table 2). Very little dimer "b" was found, but there was a substantial fraction of dimer "e" (nearly as much as in WT) (Table 2). Unlike E94A, even at 2 min, about 20% of the iron gave a magnetically split spectrum, "d", at 4.1 K, which was evident even on the small velocity scale. In this variant the parameters of doublets "e" could clearly be distinguished from those of clusters "a" at 90 K (Table 1). The percentage of iron in monomers, "c", was approximately the same as in WT (25−30%). At higher loading, in contrast to WT which gave no Fe(II) at 2−3 min, when 96 or 144 Fe atoms/molecule were added to E17A,

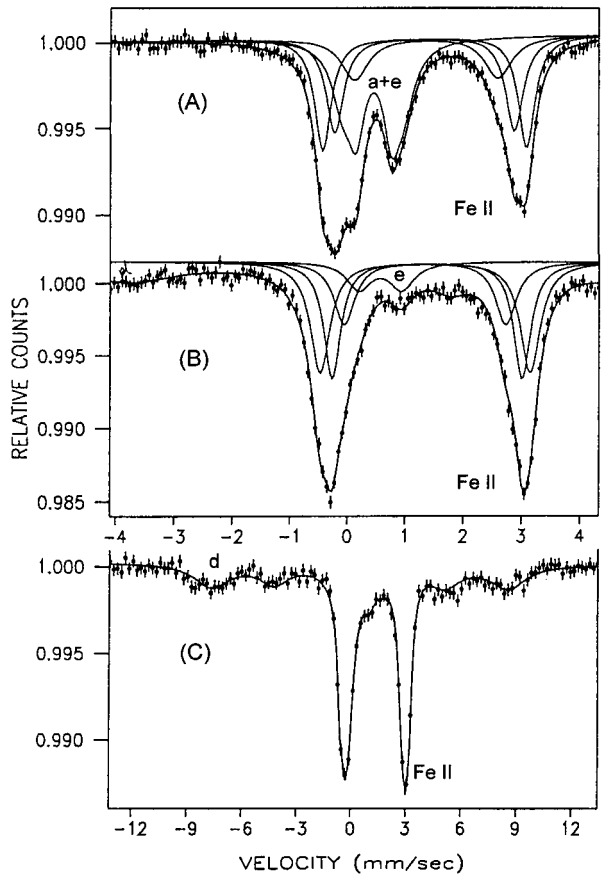

FIGURE 7: Spectra obtained at 90 K (A) and 4.1 K (B and C), in E50A frozen 1 min after addition of 48 Fe atoms/molecule. Subspectrum "a" is split at 4.1 K into sextet "d" showing clusters at t_f = 1 min, with most of the iron still not oxidized (Fe(II)).

oxidation was incomplete at 15 min (e.g., with 144 Fe, half of the iron remained unoxidized; Table 3). With 144 Fe atoms/molecule, the observed movement between 15 min and 24 h was from Fe(II) to cluster. It is not clear from the data whether this slow oxidation had occurred at the dinuclear center or directly on the growing iron core. (Iron oxidation on the surface of iron core particles has previously been postulated to occur in several ferritins (see refs *1*, and references therein, and *17*).)

(c) Variant E50A. Substitution of the bridging ligand yields an effect on Fe(II) oxidation that is intermediate between E94A and E17A (Table 2 and Figure 7). At 1 min half the iron gives three Fe(II) doublets with QS = 3.45 and IS = 1.37 mm/s, QS = 3.08 and IS = 1.37 mm/s, and QS = 2.38 and IS = 1.46 mm/s (Figure 7). The parameters of the first Fe(II) are similar to those of free Fe(II) in solution, whereas the other two Fe(II) doublets may represent Fe(II) bound to the protein. Their parameters are different from those obtained with E94A, indicating changes in the Fe(II) binding sites. At a loading of 48 Fe atoms/molecule there were no dimers "b" within the 1 h period examined and very few dimers '"e". In contrast, there was a marked tendency to cluster formation with 60% in magnetic clusters at 1 h, even though oxidation was incomplete. Remarkably, at 10 s (6 °C, 1 mM Fe), when 75% of the iron was not oxidized, 8% was in clusters. With 96 Fe atoms/molecule no subspectra "b" or "e" were seen with this variant

(d) Variant Y24F. This substitution caused a decrease in the rate of Fe(II) oxidation, as has been observed previously with this (*16*, *17*) and other ferritins (*9*, *11*). In other respects, with 48 Fe atoms/molecule, the distribution of Fe(III) species is very similar to that found with WT, although there was less dimer "b" and more dimer "e" at 1 min. The change from dimer "b" to "e" with time was not observed in this variant, and there was very little change in the species distribution within 24 h (Table 2). With 96 and 144 Fe atoms/molecule (Table 3) a trend could be seen over time, indicating that iron from both types of dimer moved to clusters. Although site C remained filled throughout all times examined, it is possible that iron passes through site C rather than moving directly from dimers to clusters. Total iron attributed to dimers never exceeded the capacity of the di-iron centers (48 Fe atoms/molecule).

(e) Variant E130A. As indicated in Figure 1, Glu130 is able to bind iron at both sites B and C, forming a long carboxylate bridge between them (Stillman, Artymiuk, and Harrison, unpublished observation). Loss of Glu130, unlike Glu94, seems to have very little effect on the rate of Fe(II) oxidation, which is complete at 10 s (6 °C, 1 mM Fe) as in WT (Table 2). However, E130A is dramatically different from WT in three respects: in the properties of dimers "e", in the decrease in monomer "c", and in the greatly increased drive toward cluster formation (Tables 2 and 3). The QS of "e" is larger than that of "e" in WT (Table 1) and, as mentioned above, the asymmetry of spectra obtained at 90 K indicates a much weaker coupling between the two iron atoms in this "e" dimer. There are fewer monomers than with WT at short times (t_f < 1 min) in the 1 mM Fe(II) samples and again in the 0.27 mM sample at 24 h. At the lower concentration nearly half of the iron is in large clusters at 1 h and 100% at 24 h.

Site C Variants, E49A, and E126A. Both variants share the characteristics of fast oxidation (no Fe(II) at 10 s), little or no production of monomers (none in the 0.27 mM Fe samples), and a greatly increased tendency to form clusters compared with WT (Tables 2 and 3). In these respects they show a general resemblance to E130A. However doublets "e" do not exhibit the marked asymmetry at 90 K seen with E130A. Because of the similarity of these doublets to "a", their intensity could only be determined from measurements at 4.1 K. The low amount of species "c" in the site C variants indicates that these monomers are mainly located at C, since the amino acid changes in these variants are at the inner surface and these substitutions would not be expected to produce significant structural changes within the protein shell.

Experiments with Alternate Additions of ^{57}Fe and ^{56}Fe. To investigate the fate of pre-existing iron when a second addition of iron is made to a preloaded sample, we devised a protocol in which samples already containing 48 or 144 Fe atoms/molecule were loaded, at a chosen time, with a further 48 Fe atoms/molecule and then frozen in liquid nitrogen at 1 min or 1 h. Loadings were made with either the Mössbauer-silent isotope ^{56}Fe first and ^{57}Fe as the second addition or vice versa and, in some cases, with two batches of ^{57}Fe.

Data for WT samples are shown in Table 4. The main conclusions from these experiments are the following: (1) For two additions of 48 Fe atoms/molecule the second iron addition does not displace the first. It tends to fill up vacant positions in sites A, B, and C and to build the core (compare sample 1 with 2 or 3 and 9 with 14). (2) Consistent with

previous experiments on HuHF (*7*, *8*) it is also clear that the build up of core increases with time (compare sample 4 with 5 and also 8 with 9 and 11 with 12). (This build up with time can also be seen in Table 3). (3) If 144 ^{56}Fe are already present, most of the ^{57}Fe added subsequently is found in core even at 1 min after its addition (sample 6). A change from dimer "b" to dimer "e" is also seen with time in some samples (see samples 2 and 3). As seen from Table 4, "b" plus "e" taken together (in 13 and 14, or 2 plus 8 and 4 plus 11) does not exceed 48 Fe atoms/molecule in total, consistent with both occupying the di-iron centers. Comparisons of several samples (e.g., 2 with 1, and 7 with 8) indicate the movement of iron from "e" to "d" within 1 min of the second addition.

Except for this shift it is interesting to note that the second addition of iron has little immediate effect on the first, but over 1 h there is significant movement into clusters from both dimers "b" (compare samples 8 and 9) and "e" (samples 11 and 12). This movement does not occur in the absence of the second addition and in this case must be due to the provision by clusters of sites with high affinity for Fe(III). The large amount of iron from the second addition found in clusters at 1 min suggests that some or all of it may be oxidized directly on the core surface. This would be in agreement with the relatively much slower oxidation of the second addition reported previously (*17*). Blocking of ferroxidase center sites by Fe(III) may also contribute to the loss of ferroxidase activity.

The data show little or no indication of mixing of the two batches of iron other than the addition of iron to pre-existing cores. Thus, as long as di-iron sites in WT are occupied by Fe(III) dimers, they are inactive as ferroxidase centers. The regain of oxidative activity after the oxidation of the first 48 Fe(II) atoms/molecule depends on the time taken for the ferroxidase centers to be vacated, and this was found previously to be much faster for variant E130A than for WT (*16*, *17*). This is consistent with the data presented here (Table 2). Thus in WT with 48 Fe atoms/molecule, two-thirds of the iron occupied dimer sites "b" and "e" and none was in core up to at least 24 h after the first Fe(II) addition, whereas in E130A less than one-third of the iron was in dimer sites, "b" and "e", and nearly half in core at 1 h and by 24 h all of the dimer iron had moved to core. It was also found that when 48^{57}Fe(II) atoms/molecule were added to E130A containing 144 ^{56}Fe (all in core species "d", Table 3), half of the ^{57}Fe was in dimer sites at 1 min (data not shown), whereas with WT (sample 6, Table 4) nearly all the ^{57}Fe was found in core. The data in Table 3 indicate that in this sample of WT several of the dimer sites were occupied at the time of the second addition. These experiments indicate that dimer sites that are already occupied by Fe(III) are unable to participate in the oxidation of incoming Fe(II).

DISCUSSION

Pereira et al. reported high- and low-field Mössbauer measurements of recombinant frog H ferritin (FrHF) (*15*). The Mössbauer spectra they obtained were analyzed with 3 doublets having QS of about 1.2, 1.7, and 0.7 mm/s and different intensities which were attributed to 3 different dimers. It is possible that a good fit to their spectra could also have been obtained with the first two doublets (with QS 1.2 and 1.7 mm/s) constrained to be of equal intensities, as we have found in our current analysis of similar subspectra. In this interpretation the two doublets would have arisen from the two iron atoms of a single dimer, similar to dimer "b" described here. The "0.7 doublet" observed by Pereira et al. (*15*) may be equivalent to dimer "e" described here. A similar doublet seen with both HuHF and its variants was attributed by us to small clusters (*18*). However, this too could be the equivalent of dimer "e". Since no spectra obtained at 90 K or above were shown for FrHF (*15*), no conclusion can be made as to whether this doublet shows relaxation phenomena at higher temperatures such as those observed in EcFtnA.

A broad, undefined spectrum, extending from -9 to $+9$ mm/s, was observed in FrHF at 4.2 K and was proposed to be equivalent to the slow relaxation spectrum observed in HuHF (*18*). However, whereas no relaxation spectrum was reported at 90 K in FrHF, a slow relaxation spectrum was observed at 90 K in both HuHF (*18*) and EcFtnA. At 90 K the broad spectrum in FrHF had collapsed into a doublet and was considered to be part of the doublet with QS $= 0.7$ mm/s. This is not the case either in EcFtnA or HuHF, since in these ferritins the relative intensities of the relaxation spectra were the same at both temperatures, with only a slightly slower relaxation at 4.1 K. It is therefore reasonable to assign these slow relaxation spectra in both EcFtnA and HuHF to monomeric iron (although in different locations). In FrHF the relaxation spectrum observed at 4.2 K was assigned to a trinuclear cluster. In EcFtnA and HuHF it is possible that the subspectra extending in velocities to about ± 8 mm/s at 4.1 K, which were assigned to larger clusters, may have some contribution due to small clusters giving slow relaxation spectra. However, since all of these give the same parameters at 90 K the immediate Fe(III) environment in all clusters, large or small, must be equivalent.

The new data which have been presented here for EcFtnA WT and its variants have provided further evidence for the involvement of the two iron atoms of the dinuclear iron center in the catalysis of Fe(II) oxidation. Thus variants E17A, Y24F, E50A, and E94A all gave reduced rates of Fe(II) oxidation with the changes E94A and E50A having the greatest effect (Table 2). It can also be deduced from comparison with the site C variants E49A, E126A, and E130A that relaxation subspectrum "c" in WT is due wholly or largely to Fe(III) at site C, since this subspectrum is absent or reduced with these variants (Table 2). Consistent with this conclusion is the observation that Fe(III) giving "c" never exceeds one per subunit, even when 4 or 6 Fe(III) atoms/subunit are present (Tables 3 and 4). However, it is not impossible that, for example in E94A, some dimer sites are occupied by a single Fe(III) atom (in A) and that this could contribute to "c" in this variant. The assignment of relaxation spectrum "c" to site C in WT and the interpretation of subspectra "b" and "e" as arising from two types of dimer at the ferroxidase center lead to further conclusions about the oxidation intermediates. Thus, in E49A and E126A, dimers are the only early intermediates and they account for 90% of the Fe(III) in the first 1 min (1 mM Fe). However, in WT nearly one-third of the Fe(III) is at site C, and only two-thirds are in Fe(III) dimers at 10 s (Table 2). The oxidation stoichiometry has been found to be 3.5 Fe(II)/O_2 with WT, but only 1.8 with E126A and E130A (*16*, *17*).

This finding together with the new Mössbauer data supports the view that in WT Fe(II) is oxidized at site C along with oxidation at sites A and B of the dinuclear center. This contrasts with HuHF, for which there is no indication of the involvement of a third iron in the oxidation process (*9*, *16*).

The assignment of WT subspectra "b" and "e" to two different types of dimer at the di-iron center needs further discussion. Subspectrum "b" is similar in its parameters to those of μ-oxo-bridged Fe(III) dimers found in other di-iron proteins and in model complexes (*30*) and to subspectra found in HuHF (Table 1) (*7*, *8*, *18*). The new analysis of "b" into subspectra "b_1" and "b_2", which are of equal intensity but with slightly different parameters, is consistent with their origin from the two differently coordinated sites, A and B (Figure 1). Furthermore subspectrum "b" is absent or greatly reduced when substitutions are made in the ligands of site A (E17A), site B (E94A), or both A and B (E50A) (Table 2). The proposal that subspectra "e_1" and "e_2" also arise from two Fe(III) at the ferroxidase center is new and may be controversial. The distinct parameters and the asymmetry observed at higher temperatures clearly imply that the two types of dimer are different. QS values of e_1 and e_2 (Table 1) are within the range given for μ-hydroxy di- and tri-bridged model structures (*30*). The assignment of "e" to dimers at sites A and B in WT is consistent with their presence along with "b" at 10 s after Fe(II) addition (Table 2) and with the observation that Fe(III) in both types of dimer never exceeds 48 Fe atoms/molecule (Tables 2-4). Again, in the variants examined, dimers "e" appear early either along with "b" or, in some cases (E50A, E94A), in the absence of "b". Although subspectra "e" do appear with the ferroxidase center variants, their parameters (except for those of Y24F) differ from those of WT (Table 1). Moreover, the much greater asymmetry of subspectrum "e" in E130A than in WT is consistent with the assignment of this species to sites A and B since Glu130 is a site B ligand.

Examination of the distributions of Fe species in Tables 2 and 3 shows that in WT "b" is predominant at 10 s (1 mM Fe), whereas it is equal to, or less than, "e" at 60 s. In the series containing 0.27 mM Fe added to give 48 or 96 Fe atoms/molecule, a clear trend can be seen with time (up to at least 1 h) which shows "e" increasing at the expense of "b". This is also found with 144 Fe atoms/molecule between 3 min and 24 h. This indicates either that "e" is more stable than 'b" or that there is some other driving force for the interconversion. However, in the variants, no clear "b" → "e" trend is evident. In Y24F "b" increases slightly in the first hour as the remaining Fe(II) is oxidized, suggesting that "b" is the first product, but in the variants E17A and E50A it is "e" that increases in the first hour, not "b". This could mean either that "b" is formed before "e", but is unstable, or that "e" is formed directly after oxidation and is not a product of "b" in these variants. In the three variants, E49A, E126A, and E130A, the two types of dimer decrease roughly in parallel. This seems to suggest that in the absence of Fe(III) in C, dimer "e" is less stable, but the main driving force causing dissolution of "e" is probably the formation of clusters.

A striking difference between WT and all of the variants in Table 2 is that WT with only 48 Fe atoms/molecule gives no magnetic clusters, all the iron being retained within the protein shell. Magnetic clusters "d" are seen only with larger numbers of iron atoms. For example, with 144 Fe atoms/molecule about two-thirds of the iron is in magnetic clusters by 3 min (Table 3). In the variants the situation is different. In E94A at 24 h at least one-third of the 48 Fe atoms/molecule added is in clusters "d". It is apparent that iron has moved from both "e" and "c" sites on the shell to the cavity, with the possibility that some Fe(II) has been oxidized directly on the clusters. In E50A 60% of the iron has joined clusters within 1 h, much of it coming, apparently, by direct oxidation of Fe(II) within the cavity. Curiously, in E17A, the amount of iron present in "d" remains at a constant low value both over 24 h with 48 Fe atoms/molecule and over the first 2 h with 96 Fe atoms/molecule. At the higher iron loading, WT also shows a trend toward clusters over 24 h. It is notable that the minimum number of Fe atoms in a cluster needed to give magnetic spectra is estimated to be at least 50 (*31*). Nevertheless, with E17A and E50A (Table 2) magnetic clusters have been found even though only 10−20 Fe atoms/molecule have been assigned to species "d" and in WT (Table 3) with only 30 Fe atoms/molecule in "d". It has been concluded before that there must be an uneven molecular distribution of iron atoms in HuHF (*8*) and HoSF (*20*) resulting from Fe(III) migration between molecules. Again, such migration must take place within EcFtnA preparations leading to the production of larger, more stable clusters. The finding that variants E49A, E126A, and E130A form clusters under conditions in which WT does not implies that iron occupying site C in the latter does not participate in core nucleation, and that, if anything, it retards nucleation. It seems that site C iron is relatively tightly held in WT and only the larger, more stable, cores can compete effectively for its iron (as in WT with 144 Fe atoms/molecule; Table 3). Indeed the data in Table 3 indicate that the average core size must be at least 100 Fe atoms/molecule in Y24F to win the competition against protein sites.

Another point to note about core formation is that the thermodynamic "pulling power" of clusters causes iron to be released from dimer sites. Thus, just as ferroxidase activity is prevented by continued occupation of the di-iron sites, once these have been vacated, activity can be regenerated. Following this line of argument, the data in Table 2 suggest that a more rapid regain of oxidative activity is likely for E49A, E126A, and E130A compared with WT. This has indeed been found experimentally (*16*, *17*). Thus in WT ferroxidase activity was very low when a second batch of 48 Fe(II) atoms/molecule was added at 24 h after the first. However with the site C variants, E49A and E130A, activity was regained fully within 6 h or less.

The data of Table 4 also suggest lower ferroxidase center activity for the second addition of 48 Fe atoms/molecule to WT due to occupation of di-iron sites. Comparing lines 1 and 2 the number of Fe(III) atoms in dimers is reduced from 34 to 16 at the second addition, and this number was no greater when an interval of 1 h was allowed between additions (line 4). As mentioned earlier the second lot of Fe(II) atoms either fill up vacant di-iron sites (and become oxidized) or are converted to core.

The nature of the species giving rise to subspectra "e_1" and "e_2" remains uncertain. In WT the species giving dimers "b" is probably $[H_2O{\cdot}Fe^{3+}{\cdot}O^{2-}{\cdot}Fe^{3+}]^{4+}$, and this could be converted to a monohydroxy-bridged dimer $[OH^{-}{\cdot}Fe^{3+}{\cdot}OH^{-}{\cdot}Fe^{3+}]^{4+}$ or $[H_2O{\cdot}Fe^{3+}{\cdot}OH^{-}{\cdot}Fe^{3+}]^{5+}$, respectively, by migra-

tion or addition of a proton, or to a dihydroxy-bridged dimer $[H_2O{\cdot}Fe^{3+}{\cdot}(OH^-)_2{\cdot}Fe^{3+}]^{4+}$ by addition of a water molecule.

In variants E17A, E50A, and E94A the deleted carboxyl group might be replaced by OH^- in the di-iron complex, so that a neutral dimer is formed as in WT. The formation of dimers in these variants may mean that, even though Fe(II) binding is weakened, the binding of two Fe(II) atoms in proximity, however transiently, can occur for long enough to allow a 2-electron oxidation to take place. Alternatively, Fe(II) atoms may be oxidized in two steps. For example, in E94A, Fe(II) may be bound and oxidized initially at site A alone, with the second iron, bound more weakly at site B, being oxidized in a second step.

The differences in ferroxidase activity and iron core build up between EcFtnA and HuHF are interesting. Initial oxidation of only 2 Fe(II) per oxygen molecule at the dinuclear centers of HuHF leads to the formation of peroxide, which, if released, could produce harmful hydroxyl radicals by Fenton reactions with further Fe(II) (*1*, *17*, *32*). Hence there is immediate pressure to produce ferrihydrite iron cores on the surfaces of which 4 Fe(II) are oxidized per oxygen molecule with the production of water (*1*, *9*, *32*). Thus the main function of the ferroxidase centers in HuHF may be to provide the Fe(III) for core formation. Once the iron cores are established, increasing numbers of potential iron-binding and oxidation sites become available on their surfaces and these can compete with protein sites for iron. The co-assembly in human and other animal ferritins of both H and L subunits promotes such core growth (*1*, *33*). For example, it was found in an earlier Mössbauer spectroscopic study that when 38 Fe(II) atoms were added to horse spleen ferritin (at pH 7), 90% of the iron was in the core at 3 min (*7*).

Potentially toxic mixtures of peroxide and Fe(II) are avoided in EcFtnA by oxidation of 3−4 Fe(II) atoms per oxygen molecule, three of these on protein sites, A, B, and C (most likely on the same subunit), with the possibility of a fourth Fe(II) being oxidized in solution (*10*, *17*). Although there is a greater tendency in EcFtnA than in HuHF to retain iron at sites on the protein shell, nevertheless cores are built, indicating that EcFtnA can act as an iron storage protein. Such a function was demonstrated when a second addition of 48 Fe(II) atoms was made (Table 4) or when 96 or 144 Fe(II) atoms were added together (Table 3). Thus, although the second batch of Fe(II) tended to fill vacant dimer sites, some of it was found in cores within 1 min of its addition (Table 4, lines 2 and 4) and nearly half of the original iron had moved from dinuclear sites to core by 1 h (Table 4, lines 11 and 12). Some of the dimer iron may even have been displaced by incoming Fe(II). Thus 9 dimer sites were occupied at 1 min by the labeled iron (Table 4, line 4), even though only 7 such sites were available (Table 2, 1 h data). On the other hand, comparing the data in Table 4, line 6, with the distribution of 144 Fe atoms/molecule at 24 h, it is evident that less than 2 of the 8 available dinuclear sites were occupied by the new batch of Fe(II) at 1 min and the bulk of the added iron was found in pre-existing magnetic cores. Although this iron may have been oxidized on the protein and then rapidly moved to the core, direct oxidation on the core is a possibility here.

Observations of *E. coli* and its mutants have demonstrated an iron storage role for EcFtnA during the stationary phase of growth in iron-rich media, with magnetic cores being observed by whole-cell Mössbauer spectroscopy (*34*). Under iron-restricted conditions EcFtnA is made available to enhance growth, and the greater availability of its protein-bound iron than that sequestered in core could provide some advantage under these conditions, as has been suggested before (*17*).

REFERENCES

1. Harrison, P. M., and Arosio, P. (1996) *Biochim. Biophys Acta 1275*, 161−203.
2. Hempstead, P. D., Yewdall, S. J., Fernie, A. R., Lawson, D. M., Artymiuk, P. J., Rice, D. W., Ford, G. C., and Harrison, P. M. (1997) *J. Mol. Biol. 268*, 424−448.
3. Harrison, P. M., Hempstead, P. D., Artymiuk, P. J., and Andrews, S. C. (1998) in *Metal Ions in Biological Systems* (Sigel, A., and Sigel, H., Eds.) Vol. 35, pp 435−477, Marcel Dekker Inc., New York.
4. Frolow, F., Kalb, A. J., and Yariv, J. (1994) *Nat. Struct. Biol. 1*, 453−460.
5. Hempstead, P. D., Hudson, A. J., Artymiuk, P. J., Andrews, S. C., Banfield, M. J., Guest, J. R., and Harrison, P. M. (1994) *FEBS Lett. 350*, 258−262.
6. Lawson, D. M., Artymiuk, P. J., Yewdall, S. J., Smith, J. M. A., Livingstone, J. C., Treffry, A., Luzzago, A., Levi, S., Arosio, P., Cesareni, G., Thomas, C. D., Shaw, W. V., and Harrison, P. M. (1991) *Nature 349*, 541−544.
7. Bauminger, E. R., Harrison, P. M., Hechel, D., Nowik, I., and Treffry, A. (1991) *Biochim. Biophys. Acta, 1118*, 48−58.
8. Bauminger, E. R., Harrison, P. M., Hechel, D., Hodson, N. W., Nowik, I., Treffry, A., and Yewdall, S. J. (1993) *Biochem. J. 296*, 709−719.
9. Treffry, A., Zhao, Z., Quail, M. A., Guest, J. R., and Harrison, P. M. (1995) *Biochemistry 34*, 15204−15213.
10. Treffry, A., Zhao, Z. W., Quail, M. A., Guest, J. R., and Harrison, P. M. (1997) *Biochemistry 36*, 432−441.
11. Fetter, J. Cohen, J., Danger, D., Sanders-Loehr, J., and Theil, E. C. (1997*) J. Biol. Inorg. Chem. 2*, 652−661.
12. Zhao, Z. W., Treffry, A., Quail, M. A., Guest, J. R., and Harrison, P. M. (1997) *J. Chem. Soc., Dalton Trans.*, 3977−3978.
13. Pereira, A. S., Small, W., Krebs, C., Tavanes, P., Edmondson, D. E., Theil, E. C., and Huynh, B. H. (1998) *Biochemistry 37*, 9871−9876.
14. Waldo, G. S., and Theil, E. C. (1993) *Biochemistry 32*, 13262−13269.
15. Pereira, A. S., Tavares, P., Lloyd, S. G., Danger, D., Edmondson, D. E., Theil, E. C., and Huynh, B. H. (1997) *Biochemistry 36*, 7917−7927.
16. Harrison, P. M., and Treffry, A. (1998) in *Inorganic and regulatory mechanisms of iron metabolism* (Fereira, G., Moura, J., and Franco, R., Eds.) Wiley-VCH (in press).
17. Treffry, A., Zhao, Z. W., Quail, M. A., Guest, J. R., and Harrison, P. M. (1998*) FEBS Lett. 432*, 213−225.
18. Bauminger, E. R., Treffry, A., Hudson, A. J., Hechel, D., Hodson, N. W., Andrews, S. C., Levi, S., Nowik, I., Arosio, P., Guest, J. R., and Harrison, P. M. (1994*) Biochem. J. 302*, 813−820.
19. Hudson, A. J., Andrews, S. C., Hawkins, C., Williams, J. M., Izuhara, M., Meldrim, F. C., Mann, S., Harrison, P. M., and Guest, J. R. (1993) *Eur. J. Biochem. 218*, 985−995.
20. Bauminger, E. R., Harrison, P. M., Nowik, I., and Treffry, A. (1989) *Biochemistry 28*, 5486−5493.
21. Nowik, I., and Wickman, H. H. (1966) *Phys. Rev. Lett. 17*, 949−951.
22. Goldanskii, V. I., and Makarov E. F. (1968) *in Chemical Applications of Mössbauer spectroscopy*, (Goldanskii V. I., and Herber R. H., Eds) pp 102−107, Academic Press, New York.
23. Shulman, R. G., and Wertheim, G. K. (1964) *Rev. Mod. Phys. 36*, 459.
24. Blume, M. (1967) *Phys. Rev. Lett. 18*, 305−308.

25. Silver, J., and Lukas, B. (1983) *Inorg. Chim. Acta 78*, 219−224.
26. Buckley, A. N., Wilson, G. V. H., and Murray, K. S. (1969) *Solid State Commun. 7*, 471−474.
27. Lechan, R., Nicolini, C., Abeledo, C. R., and Frankel R. B. (1973) *J. Chem. Phys. 59*, 3138−3142.
28. Buckley, A. N., Herbert, I. R., Rumbold, B. D., Wilson, G. V. H., and Murray, K. S. (1970) *J. Phys. Chem. Solids 31*, 1423−1434.
29. Goldanskii, V. I., and Makarov E. F. (1968) in *Chemical Applications of Mössbauer spectroscopy* (Goldanskii V. I., and Herber R. H., Eds.) pp 42−44, Academic Press, New York.
30. Lambert, E., Chabut, B., Chardon-Noblat, S., Deronzier A., Chottard, G., Bousseksou, A., Tuchagues, J.-P., Laugier, J., Bardet, M., and Latour, J.-M. (1997) *J. Am. Chem. Soc. 119*, 9424−9437.
31. Frankel, R. B., Papaefthymiou G. C., and Watt G. D. (1991) *Hyperfine Interact. 66*, 71−82.
32. Sun, S., Arosio, P., Levi, S., and Chasteen, N. D. (1993) *Biochemistry 32*, 9362−9369.
33. Santambrogio, P., Levi, S., Cozzi, A., Corsi, B., and Arosio, P. (1996) *Biochem. J. 314*, 139−144.
34. Abdul-Tehrani, H., Hudson, A. J., Chang, Y.-S., Timms, A. R., Hawkins, C., Williams, J. M., Harrison, P. M., Guest, J. R., and Andrews, S. C. (1999) *J. Bacteriol. 181*, 1415−1428.

BI990377L